Graph-Based User Scheduling Algorithms for LEO-MIMO Non-Terrestrial Networks

Graph-Based User Scheduling Algorithms for LEO-MIMO Non-Terrestrial Networks

Bilal Ahmad*, Daniel Gaetano Riviello*, Alessandro Guidotti†, Alessandro Vanelli-Coralli*
*Department of Electrical, Electronic, and Information Engineering (DEI), University of Bologna, Bologna, Italy
†National Inter-University Consortium for Telecommunications (CNIT), Bologna, Italy
{bilal.ahmad6, daniel.riviello, a.guidotti, alessandro.vanelli}@unibo.it

***Abstract*—In this paper, we study the user scheduling problem in a Low Earth Orbit (LEO) Multi-User Multiple-Input-Multiple-Output (MIMO) system. We propose an iterative graph-based maximum clique scheduling approach, in which users are grouped together based on a dissimilarity measure and served by the satellite via space-division multiple access (SDMA) by means of Minimum Mean Square Error (MMSE) digital beamforming on a cluster basis. User groups are then served in different time slots via time-division multiple access (TDMA). As dissimilarity measure, we consider both the channel coefficient of correlation and the users' great circle distance. A heuristic optimization of the optimal cluster size is performed in order to maximize the system capacity. To further validate our analysis, we compare our proposed graph-based schedulers with the well-established algorithm known as Multiple Antenna Downlink Orthogonal clustering (MADOC). Results are presented in terms of achievable per-user capacity and show the superiority in performance of the proposed schedulers w.r.t. MADOC.**

***Index Terms*—LEO, MU-MIMO, User Scheduling, Beamforming, MMSE**

I. Introduction

Future 6G communication networks are expected to be able to provide connectivity to an extremely large number of devices at high throughput with minimal delay. LEO Non-Terrestrial Networks (NTN) systems are expected to be a game changer thanks to their less stringent requirements in terms of power consumption and propagation delay w.r.t. the Geostationary Earth Orbit (GEO) counterpart. Also, Massive MIMO has emerged as a key enabler for NTN. It has the ability to boost the spectral efficiency, increase the available degrees of freedom, and achieve high data speeds. With the application of cutting-edge digital beamforming algorithms, a LEO satellite with an antenna array and a large number of antenna elements can provide service to many user terminals (UTs) in full frequency reuse (FFR) schemes. Both GEO and LEO NTN systems have received substantial attention with regard to the application of such approaches. The objective has been to increase the total throughput in unicast or multicast systems while solving other crucial problems for NTN-based beamforming, such as user scheduling or user grouping and retrieval of Channel State Information (CSI) [1]–[5]. Specifically, Minimum Mean Square Error (MMSE) digital beamforming, also known as Regularized Zero Forcing [6], is a common pre-processing technique for real systems because of its low complexity as well as its capability to completely mitigate interference.

Given the extremely large number of UTs on the ground w.r.t. the antennas available on the satellite, the design of a proper user scheduling strategy becomes crucial. Scheduling can be accomplished by grouping users into different clusters: i) users within the same cluster are multiplexed and served together via space-division multiple access (SDMA), i.e., digital beamforming or Multi-User MIMO (MU-MIMO) techniques; ii) the different clusters of users are then served on different time slots via time-division multiple access (TDMA) [2], [3]. The design of an optimal user grouping strategy is known to be an NP-complete problem which can be solved only through exhaustive search [7]. In [3], a greedy user scheduling strategy for downlink MU-MIMO has been proposed. The authors take into account heterogeneous users and suggest two hybrid user scheduling algorithms that can capture user fairness while maximizing sum-rate capacity in a greedy manner. Multiple antenna downlink orthogonal clustering (MADOC), a well established low complexity algorithm introduced in [8], expands on the work in [3] and considers user fairness and group number minimization into account.

In this paper, we extend our work in [9] by proposing a low-complexity graph-based framework for user scheduling for MU-MIMO LEO NTN systems aiming at maximizing the sum-rate capacity of the system while preserving fairness among the users. We model the clustering problem as an undirected and unweighted graph: each vertex represents a UT, while the edges of the graph are based on one of the two possible dissimilarity measures:

1) an edge in the graph between 2 users exists if their channel coefficient of correlation (CoC), as defined in [8] is below a certain threshold,
2) an edge in the graph between 2 users exists if their great-circle distance is above a certain threshold.

It is clear that the first scheduling method requires CSI availability at the transmitter during the scheduling phase, while the second method requires only the knowledge of users' positions. Once defined the graph, at each step, the procedure searches for the maximum clique, i.e., the largest fully connected subgraph in the graph through the efficient MaxCliqueDyn algorithm [10]. The vertices belonging to that clique are assigned to a cluster, removed from the graph and the procedure is repeated until there are no more users to schedule. For each cluster, SDMA is accomplished by

means of feed space MMSE beamforming, furthermore, we consider two different types of power normalization of the beamforming matrix: Sum Power Constraint (SPC) and Maximum Power Constraint (MPC) [11]. A heuristic optimization of the graph thresholds is performed for both approaches so that the system's overall capacity is maximized. With the aim of validating our analysis, the results are compared with the MADOC algorithm and with a position-based scheduler, in which a beam lattice is generated on-ground and one user per beam is randomly selected to form a cluster.

II. System Model

A Single Multi-beam (MB) LEO satellite equipped with an on-board planar antenna array is considered here. The antenna array consists of N radiating elements which provide connectivity to a total of K single-antenna uniformly distributed on-ground users by means of $S \leq N$ beams. Our further assumptions are based on the system architecture comprehensively explained in [2], [9]. The on-ground gNB is responsible for the user grouping, i.e., Radio Resource Management (RRM) and computation of the beamforming coefficients. Both scheduling and beamforming require the estimation of CSI which is provided by the UTs. The CSI values are computed by the users at time instant t_0; the scheduling and the beamforming matrices for every group of users are then computed at the gNB and, finally, actually used to transmit the beamformed symbols to the users at time $t_0 + \Delta t$. The latency Δt between the channel estimation phase and the transmission phase introduces a misalignment between the channel on which the scheduling and the beamforming matrices are computed and the actual channel through which the transmission occurs, which impacts the system performance. The latency is due to

$$\Delta t = t_{ut,max} + 2t_{feeder} + t_p + t_{ad} \tag{1}$$

where i) $t_{ut,max}$ is the maximum propagation delay for the UTs requesting connectivity in the coverage area; ii) t_{feeder} is the propagation delay on the feeder link, considered twice since the estimates are to be sent to the GW on the return link and then the beamformed symbols are sent on the forward link to the satellite; iii) t_p is the processing delay needed to compute the beamforming matrix; and iv) t_{ad} includes any additional delay. The antenna array model assumed here is based on ITU-R Recommendation M.2101 [13] illustrated in Fig. 1.

By default, the antenna boresight direction is defined by the direction of the Sub-Satellite Point (SSP). The point P is the position of the user terminal on the ground. The user directions are identified by (ϑ, φ) angles where the boresight direction is (0,0). We can now derive the direction cosines for the considered user as $u = \frac{P_y}{\|P\|} \sin\vartheta \sin\varphi$, and $v = \frac{P_z}{\|P\|} \cos\vartheta$. The total array response of the Uniform Planar Array (UPA) in the generic direction (ϑ_i, φ_i) can be expressed as the Kronecker product of the array responses of the 2 Uniform Linear Arrays (ULAs) lying on the y- and z-axis [14], [15]. We first define the $1 \times N_H$ steering vector (SV) of the ULA

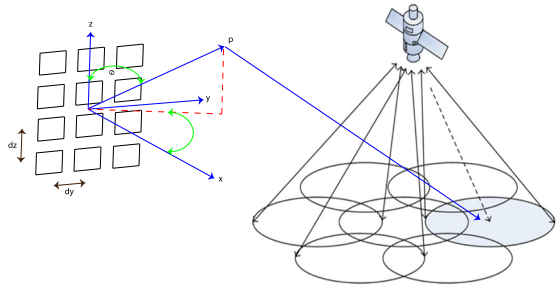

Fig. 1: Multi-beam Antenna Array Model from ITU-R M.2101-0. [13]

along the y-axis $\mathbf{a}_H(\theta_i, \varphi_i)$ and the $1 \times N_V$ SV of the ULA along the z-axis $\mathbf{a}_V(\theta_i)$:

$$\mathbf{a}_H(\vartheta_i,\varphi_i) = \left[1, e^{jk_0 d_H \sin\vartheta_i \sin\varphi_i}, \ldots, e^{jk_0 d_H (N_H-1) \sin\vartheta_i \sin\varphi_i}\right] \tag{2}$$

$$\mathbf{a}_V(\vartheta_i) = \left[1, e^{jk_0 d_V \cos\vartheta_i}, \ldots, e^{jk_0 d_V (N_V-1) \cos\vartheta_i}\right]. \tag{3}$$

Where $k_0 = 2\pi\lambda$ is the wave number, N_H, N_V denotes the number of array elements on the horizontal (y-axis) and vertical (z-axis) directions with $N = N_H \cdot N_V$ and d_H, d_V denote the distance between adjacent array elements on the y- and z-axis respectively. We assume that the array is equipped with directive antenna elements, whose radiation pattern is denoted by $g_E(\vartheta_i, \varphi_i)$. Finally, we can express the $1 \times N$ SV of the UPA at the satellite targeted for the i-th user as the Kronecker product of the 2 SV's along each axis multiplied by the element radiation pattern:

$$\mathbf{a}(\vartheta_i, \varphi_i) = g_E(\vartheta_i, \varphi_i)\, \mathbf{a}_H(\vartheta_i, \varphi_i) \otimes \mathbf{a}_V(\vartheta_i) \tag{4}$$

The CSI vector at feed level $\hat{\mathbf{h}}_i$ represents the channel between the N radiating elements and the generic i-th on-ground UT, with $i = 1, \ldots, K$, can be written as:

$$\hat{\mathbf{h}}_i = G_i^{(rx)} \frac{\lambda}{4\pi d_i} \sqrt{\frac{L_i}{\kappa B T_i}} e^{-j\frac{2\pi}{\lambda} d_i} \mathbf{a}(\vartheta_i, \varphi_i) \tag{5}$$

in which, d_i is the slant range between the generic i-th user and the satellite, λ is the wavelength, $\kappa B T_i$ denotes the equivalent thermal noise power, with κ being the Boltzmann constant, B the user bandwidth (assumed to be the same for all users), and T_i the equivalent noise temperature of the i-th UT. $G_i^{(rx)}$ denotes the receiving antenna gain for the i-th UT, while L_i denotes all the additional losses per user, such as for example atmospheric, antenna, and cable losses. More in detail, the additional losses are computed based on 3GPP TR 38.821 [12] as

$$L_i = L_{sha,i} + L_{atm,i} + L_{sci,i} \tag{6}$$

where $L_{sha,i}$ represents the log-normal shadow fading term, $L_{atm,i}$ the atmospheric loss, and $L_{sci,i}$ the scintillation. Collecting all of the K CSI vectors, it is possible to build a $K \times N$ complex channel matrix at system level $\hat{\mathbf{H}} = \left[\hat{\mathbf{h}}_1^\intercal, \hat{\mathbf{h}}_2^\intercal, \ldots, \hat{\mathbf{h}}_K^\intercal\right]^\intercal$, where the generic k-th row contains the

CSI vector of the k-th user and the generic n-th column contains the channel coefficients from the n-th on-board feed towards the K on-ground users.

Given the set of all users to be scheduled, denoted with $\mathcal{U} = \{U_1, U_2, \ldots, U_K\}$, the Radio Resource Management (RRM) algorithm defines a possible users' partitioning $\{\mathcal{C}_1, \mathcal{C}_2, \ldots, \mathcal{C}_P\}$ where $\mathcal{C}_p \subseteq \mathcal{U}$ is defined as cluster and $|\mathcal{C}_p| = K_p$ is defined as the cardinality of the p-th cluster with $p = 1, \ldots, P$. Clusters are not necessarily disjoint sets of users, clearly $|\mathcal{C}_1 \cup \mathcal{C}_2 \cup \ldots \cup \mathcal{C}_P| = K$. In each time slot, users belonging to cluster $\mathcal{C}_p$ are selected, leading to a $K_p \times N$ complex scheduled channel matrix $\hat{\mathbf{H}}_p \subseteq \hat{\mathbf{H}}$, which contains only the rows of the scheduled users in the p-th cluster. The selected beamforming algorithm computes for each cluster a $N \times K_p$ complex beamforming matrix $\mathbf{W}_p = [\mathbf{w}_1^{(p)}, \mathbf{w}_2^{(p)}, \ldots, \mathbf{w}_{K_p}^{(p)}]$, where $\mathbf{w}_i^{(p)}$ denotes the $N \times 1$ beamformer designed for the i-th user in the p-th cluster. The matrix $\mathbf{W}_p$ projects the K_p dimensional column vector $\mathbf{s}_p = [s_1, s_2, \ldots, s_{K_p}]^\intercal$ containing the unit-variance user symbols onto the N-dimensional space defined by the antenna feeds. Thus, in the feed space, the computation of the beamforming matrix allows for the generation of a dedicated beam towards each user direction. The signal received by the i-th user in the p-th cluster can be expressed as follows [9]:

$$y_k^{(p)} = \mathbf{h}_k \mathbf{w}_k^{(p)} s_k + \sum_{\substack{i=1 \\ i \neq k}}^{K_p} \mathbf{h}_k \mathbf{w}_i^{(p)} s_i + z_k^{(p)} \tag{7}$$

where $z_k^{(p)}$ is a circularly symmetric Gaussian random variable with zero mean and unit variance. The K_p-dimensional vector of received symbols in the p-th cluster is:

$$\mathbf{y}_p = \mathbf{H}_p \mathbf{W}_p \mathbf{s}_p + \mathbf{z}_p \tag{8}$$

It shall be noted that, as previously discussed, the estimated channel matrix $\hat{\mathbf{H}}$ at time t_0 is used to compute the scheduling and the beamforming matrices $\mathbf{W}_p$ in the estimation phase, while the beamformed symbols are sent to the users at a time instant $t_0 + \Delta t$, in which the scheduled channel matrices and vectors are different and denoted as $\mathbf{H}_p$ and $\mathbf{h}_k$, respectively.

The Signal-to-Interference-plus-Noise ratio (SINR) for user k belonging to cluster p can be computed as

$$\text{SINR}_k^{(p)} = \frac{\left\| \mathbf{h}_k \mathbf{w}_k^{(p)} \right\|^2}{1 + \sum\limits_{\substack{i=1 \\ i \neq k}}^{K_p} \left\| \mathbf{h}_k \mathbf{w}_i^{(p)} \right\|^2} \tag{9}$$

Given a TDMA time frame T_F, each cluster is assigned a time slot T_p. In order to design a fair-proportional scheduler, we assume that we can adjust the duration of each time slot T_p to be proportional to the cardinality of each cluster K_p, i.e.,

$$\begin{aligned} T_p &= \gamma_p T_F \\ \gamma_p &= \frac{K_p}{\sum_{p=1}^{P} K_p} \end{aligned} \tag{10}$$

Therefore, in order to take into account the duty cycle associated with each cluster, we can define the per-user achievable capacity as:

$$C_k = B \sum_{\substack{p \\ U_k \in \mathcal{C}_p}} \gamma_p \log_2 \left(1 + \text{SINR}_k^{(p)}\right) \tag{11}$$

where γ_p denotes the cluster weight. The beamforming matrix $\mathbf{W}_p$, which is computed on a cluster basis, is based on the linear Minimum Mean Square Error (MMSE) equation:

$$\mathbf{W}_p = \hat{\mathbf{H}}_p^H (\hat{\mathbf{H}}_p \hat{\mathbf{H}}_p^H + \alpha \mathbf{I}_{K_p})^{-1} \tag{12}$$

where $\mathbf{I}_{K_p}$ indicates the $K_p \times K_p$ identity matrix and $\alpha = \frac{N}{P_t}$ is the regularisation factor with P_t the total on-board power. Finally, as detailed in [1], [9], the power normalization is a fundamental step for beamforming so as to properly take into account the power that can be emitted both by the satellite and per antenna. We consider the following two options for power normalization i.e. Sum Power Constraint (SPC), Maximum Power Constraint (MPC) defined as:

$$\text{SPC} \longrightarrow \tilde{\mathbf{W}}_p = \frac{\sqrt{P_t}\mathbf{W}_p}{\sqrt{\text{tr}(\mathbf{W}_p \mathbf{W}_p^H)}} \tag{13}$$

$$\text{MPC} \longrightarrow \tilde{\mathbf{W}}_p = \frac{\sqrt{P_t}\mathbf{W}_p}{\sqrt{N \max_j \left[\mathbf{W}_p \mathbf{W}_p^H\right]_{j,j}}} \tag{14}$$

III. Graph-based user scheduling

We denote with $\mathcal{G} = (\mathcal{V}, \mathcal{E})$ an undirected and unweighted graph with vertex set $\mathcal{V}$ and edge set $\mathcal{E}$. A clique $\mathcal{Q}$ of $\mathcal{G}$ is a subset of the vertices, $\mathcal{Q} \subseteq \mathcal{V}$, such that every two distinct vertices are adjacent, i.e., $\mathcal{Q}$ is a complete subgraph. In our LEO NTN MIMO scenario, the set of vertices $\mathcal{V}$ coincides with the set of users $\mathcal{U}$ and the edge set is constructed based on a dissimilarity measure, which can be one of the following:

1) In case of CSI availability at the transmitter at the scheduling phase, we can adopt as a dissimilarity measure the channel CoC [16], defined as:

$$[\mathbf{\Psi}]_{i,j} = \frac{\left| \hat{\mathbf{h}}_i \hat{\mathbf{h}}_j^H \right|}{\left\| \hat{\mathbf{h}}_i \right\| \left\| \hat{\mathbf{h}}_j \right\|} \tag{15}$$

where $[\mathbf{\Psi}]_{i,j} \in [0, 1]$. The set of edges $\mathcal{E}$ of the $\mathcal{G}$ graph is completely determined by its adjacency matrix $\mathbf{A}$, whose entries are defined as:

$$[\mathbf{A}]_{i,j} = \begin{cases} 1, & [\mathbf{\Psi}]_{i,j} \leq \delta_C \\ 0, & [\mathbf{\Psi}]_{i,j} > \delta_C \end{cases} \tag{16}$$

where δ_C denotes a properly designed threshold. If an element of $\mathbf{A}$ is equal to 0, $\mathbf{h}_i$ and $\mathbf{h}_j$ are considered to be co-linear and there is no edge between U_i and U_j, while if an element of $\mathbf{A}$ is equal to 1, $\mathbf{h}_i$ and $\mathbf{h}_j$ are considered to be orthogonal, i.e., there is an edge between U_i and U_j and they can belong to the same cluster.

2) In case of no CSI availability at the transmitter at the scheduling phase, when only users' positions are known,

we can adopt as dissimilarity measure the users' great circle distance. Given the latitudes, ϕ_i and ϕ_j of the users i and j, respectively, and λ_i and λ_j their respective longitudes, their great circle distance can be computed through the haversine formula. We first define:

$$h = \sin^2\left(\frac{\phi_j - \phi_i}{2}\right) + \cos\phi_i \cdot \cos\phi_j \cdot \sin^2\left(\frac{\lambda_j - \lambda_i}{2}\right) \tag{17}$$

then

$$[\mathbf{\Gamma}]_{i,j} = 2r \arcsin\left(\sqrt{h}\right) \tag{18}$$

We can define now the corresponding adjacency matrix $\mathbf{A}$ as:

$$[\mathbf{A}]_{i,j} = \begin{cases} 1, & [\mathbf{\Gamma}]_{i,j} \geq \delta_D \\ 0, & [\mathbf{\Gamma}]_{i,j} < \delta_D \end{cases} \tag{19}$$

where δ_D is again a properly designed threshold. If an element of $\mathbf{A}$ is equal to 1, the great-circle distance and therefore the angular distance between U_i and U_j is such that their directions (ϑ_i, φ_i) and (ϑ_j, φ_j) can be spatially separated by means of MMSE digital beamforming, and they can belong to the same cluster (or they can be co-scheduled), while if an element of $\mathbf{A}$ is equal to 0, the directions of U_i and U_j are considered to be too close to be spatially distinguished by the beamformer.

The threshold determines an upper bound on the size of a clique and therefore the optimal number of users that can be efficiently multiplexed in the space domain by MMSE beamforming within a cluster.

A maximum clique $\mathcal{Q}_{\max} \subseteq \mathcal{V}$ is a clique, such that there is no clique with more vertices. The proposed user scheduling algorithm is a greedy iterative procedure that aims at minimizing the total number of clusters P, given an optimized threshold δ_C for the CSI-based case or δ_D for the distance-based case. This is accomplished by:

1) maximizing the size of each cluster by iteratively finding the maximum clique of the updated graph;
2) creating disjoint sets of scheduled users, i.e., $\mathcal{C}_i \cap \mathcal{C}_j = \varnothing, \ \forall i, j$, which also minimizes the total number of clusters P.

The maximum clique problem has been widely investigated in literature [17]. Several algorithms have been proposed for the exact solution of the problem, but also various efficient heuristic algorithms have been developed, which allow to solve the problem in polynomial time [18], [19]. In this work, we adopted MaxCliqueDyn [10], an efficient branch-and-bound algorithm for finding the maximum clique. An extensive computational analysis on MaxCliqueDyn and its variants can be found in [17].

As illustrated in Algorithm 1, the iterative procedure searches for the maximum clique $\mathcal{Q}_{\max}$ in the graph and declares it as a cluster; at each step, the nodes in $\mathcal{Q}_{\max}$ and any edges connected to them are removed, the graph is updated after pruning. The procedure is repeated until there are no more vertices in the graph. Fairness is guaranteed among users by setting the cluster weight $\gamma_p = \frac{K_p}{K}$, which defines the duration of the time slot T_p assigned to cluster $\mathcal{C}_p$ within the total TDMA time frame T_F.

Algorithm 1 Iterative Graph-based user scheduling algorithm

Input: Adjacency matrix $\mathbf{A}$ associated to graph $\mathcal{G}(\mathcal{U}, \mathcal{E})$
Output: Cluster sets $\mathcal{C}_p$ and cluster weights γ_p for $p = 1, \ldots, P$

```
Initialize p = 1
while U ≠ ∅ do
    Q_max = MaxCliqueDyn(G)
    C_p ← Q_max and K_p ← |C_p|
    Remove all edges E associated with vertices Q_max
    U ← U − Q_max and update G
    p ← p + 1
end while
for p:=1 to P do
    γ_p ← K_p / (Σ_{p=1}^{P} K_p)
end for
```

IV. Benchmark algorithms: MADOC and position-based random scheduler

MADOC is an efficient CSI-based scheduler presented in [8], which uses the same channel CoC in (15) as a grouping indicator. The key idea in the MADOC procedure is to use the channel CoC as a group policy and to assemble so-called ϵ-orthogonal user groups, this means that the CoC calculated for all combinations of users inside a cluster does not exceed a certain threshold ϵ. The optimal value for the threshold ϵ of MADOC depends on the scenario characteristics and hence, it has been newly identified w.r.t. [8].

A position-based scheduler is also used as a benchmark algorithm for comparison. It is a simple scheduling procedure in which a beam lattice is generated on-ground and one user per beam is randomly selected to form a cluster.

V. Simulation setup and results

TABLE I: Simulation parameters.

Parameter	Value
Carrier frequency	2 GHz
System band	S (30 MHz)
Beamforming space	feed
Receiver type	VSAT
Receiver antenna gain	39.7 dBi
Noise figure	1.2 dB
Propagation scenario	Line of Sight
System scenario	urban
Total on-board power density, $P_{t,\text{dens}}$	4 dBW/MHz
Number of tiers	5
User density	0.1 user/km^2
Cluster size for position-based scheduler	91
Number of transmitters N	1024 (32×32 UPA)
Monte Carlo iterations	100

In this section, we present the outcomes of the extensive numerical simulations with the parameters specified as in Tab. I. The assessment has been performed in full buffer conditions. A single LEO satellite is considered at a distance of 600 Km from the Earth. On average the total number of

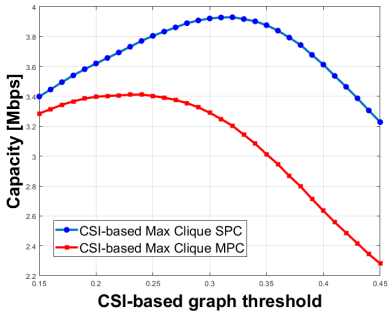

(a) CSI-based Max Clique Scheduler.

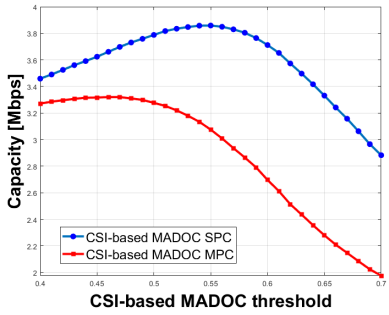

(b) CSI-based MADOC Scheduler.

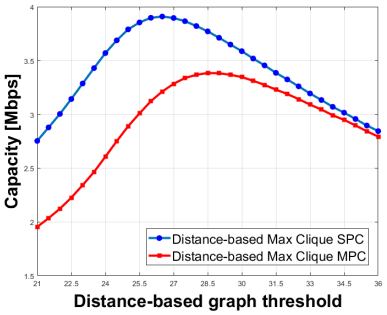

(c) Distance-based Max Clique Scheduler.

Fig. 2: Threshold optimization for graph-based and MADOC schedulers.

users are $K_T = 5700$. The satellite is equipped with a UPA of 32×32 feeds. The user terminals are fixed and their receiver antenna gain $G_{\max}^{(rx)}$ is set to 39.7 dBi. The propagation scenario is the Line of Sight model based on TR 38.811 [12] and TR 38.821 [13].

Aiming at maximizing the average per-user capacity, we performed a heuristic optimization of thresholds δ_C, ϵ and δ_D for CSI-based maximum (Max) clique, MADOC, and distance-based Max clique schedulers, respectively, as illustrated in Fig. 2 for both MMSE with SPC and MPC power normalizations. In particular, we investigate the trade-off between the maximization of the cluster size K_p (minimization of the number of clusters), and the maximization of the average per-cluster SINR, $\frac{1}{K_p}\sum_{k=1}^{K_p} \text{SINR}_k^{(p)}$, which depends on the interference rejection capability of the per-cluster MMSE beamforming matrix $\mathbf{W}_p$, i.e., the ability to separate users only in the spatial domain. Tab. II reports for each scheduler the obtained optimal threshold, the mean cluster size and the average per-user capacity, which has been computed with a per-cluster MMSE beamforming matrix with SPC and MPC normalizations. We recall that in the simulated scenario, with a Tier 5 beam lattice, the cluster size for the position-based random scheduler remains constant $K_p = 91, \forall p$. Fig. 3 shows the average per-user capacity as a function of the mean cluster size, it can be noticed that both graph-based schedulers outperform MADOC and that in general SPC normalization can offer a larger user group size w.r.t. MPC. It is worth remarking that also a non-CSI-based technique, i.e., the distance-based Max clique scheduler, can be highly competitive, although CSI knowledge at the transmitter will be required at the transmission phase on a cluster level only.

TABLE II: Simulation Results for Threshold Optimization

Parameters		CSI-based Max clique	CSI-based MADOC	Distance-based Max clique	Position-based random
Optimized threshold	SPC	0.32	0.55	26.50	-
	MPC	0.24	0.47	28.50	-
Mean cluster size	SPC	51	59.4	52.3	91
	MPC	44	50	46	91
Capacity (Mbps)	SPC	3.92	3.85	3.90	2.58
	MPC	3.41	3.32	3.38	1.77

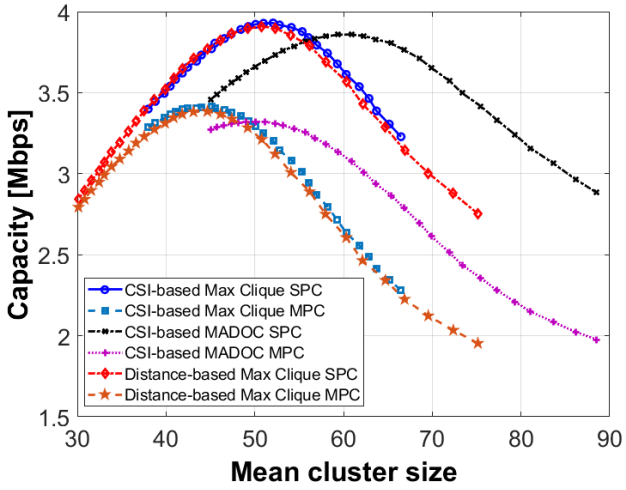

Fig. 3: Mean cluster size vs. capacity for graph-based and MADOC schedulers.

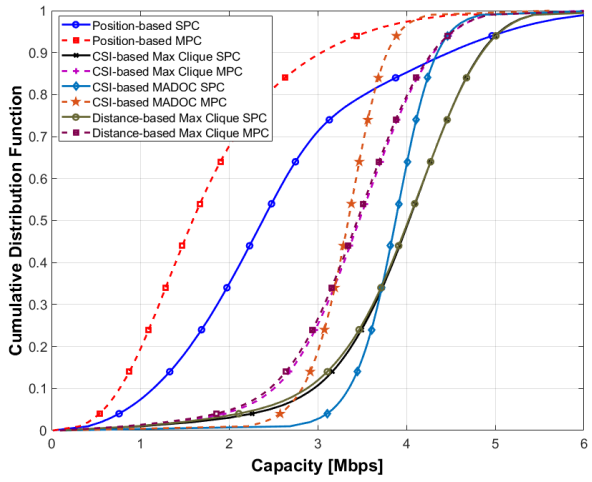

Fig. 4: CDF of users' capacity.

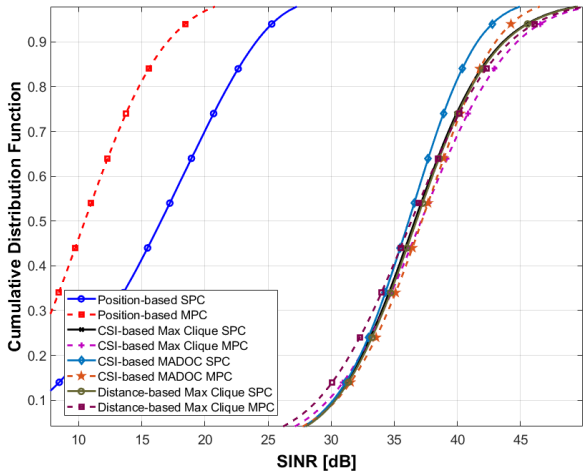

Fig. 5: CDF of users' SINR.

In Fig. 4 we show the Cumulative Distribution Function (CDF) of the user's capacity for all the considered schedulers. The CSI-based (distance-based) Max clique scheduler shows an improvement w.r.t. MADOC in terms of the average per-user capacity of approximately 0.15 (0.14) Mbps for SPC and 0.12 (0.1) Mbps for MPC. The improvement of both graph-based schedulers w.r.t. the position-based random scheduler is above 1.6 Mbps for SPC and above 1.8 Mbps for MPC. Finally, Fig 5 shows the CDF of users' SINR and further demonstrates the very high performance of both graph-based schedulers w.r.t position-based, with a slight improvement also w.r.t. to MADOC.

VI. Conclusion

We have proposed an iterative user scheduling procedure based on the maximum clique algorithm. As a grouping indicator, we have presented the channel CoC in case of CSI availability at the scheduling phase, or the users' great circle distance in case only users' locations are known. For each cluster, a digital MMSE beamforming matrix allows to spatially separate the scheduled users and we have considered two power normalizations for the MMSE matrix: SPC and MPC. We have found the optimal threshold values for both graph-based schedulers and for MADOC. The results have been presented in terms of achievable per-user capacity and SINR and show an improvement in the performance of both graph-based schedulers w.r.t. MADOC.

VII. Acknowledgments

This work has been funded by the European Union Horizon-2020 Project DYNASAT (Dynamic Spectrum Sharing and Bandwidth-Efficient Techniques for High-Throughput MIMO Satellite Systems) under Grant Agreement 101004145. The views expressed are those of the authors and do not necessarily represent the project. The Commission is not liable for any use that may be made of any of the information contained therein.

References

[1] A. Guidotti, C. Amatetti, F. Arnal, B. Chamaillard and A. Vanelli-Coralli, "Location-assisted precoding in 5G LEO systems: architectures and performances," *2022 Joint European Conference on Networks and Communications and 6G Summit (EuCNC/6G Summit)*, 2022, pp. 154-159, doi: 10.1109/EuCNC/6GSummit54941.2022.9815611.

[2] A. Guidotti and A. Vanelli-Coralli, "Clustering strategies for multicast precoding in multibeam satellite systems", *International Journal of Satellite Communications and Networking*, vol. 38, no. 2, pp. 85–104, 2020.

[3] X. Yi and E. K. S. Au, "User Scheduling for Heterogeneous Multiuser MIMO Systems: A Subspace Viewpoint", in *IEEE Transactions on Vehicular Technology*, vol. 60, no. 8, pp. 4004-4013, Oct. 2011, doi: 10.1109/TVT.2011.2165976.

[4] L. You, K. -X. Li, J. Wang, X. Gao, X. -G. Xia and B. Ottersten, "Massive MIMO Transmission for LEO Satellite Communications," in *IEEE Journal on Selected Areas in Communications*, vol. 38, no. 8, pp. 1851-1865, Aug. 2020, doi: 10.1109/JSAC.2020.3000803.

[5] M. R. Dakkak, D. G. Riviello, A. Guidotti and A. Vanelli-Coralli, "Evaluation of MU-MIMO Digital Beamforming Algorithms in B5G/6G LEO Satellite Systems," *2022 11th Advanced Satellite Multimedia Systems Conference and the 17th Signal Processing for Space Communications Workshop (ASMS/SPSC)*, 2022, pp. 1-8, doi: 10.1109/ASMS/SPSC55670.2022.9914720.

[6] E. Lagunas, A. Pérez-Neira, M. A. Lagunas and M. A. Vazquez, "Transmit Beamforming Design with Received-Interference Power Constraints: The Zero-Forcing Relaxation," *ICASSP 2020 - 2020 IEEE International Conference on Acoustics, Speech and Signal Processing (ICASSP)*, Barcelona, Spain, 2020, pp. 4727-4731, doi: 10.1109/ICASSP40776.2020.9053471.

[7] E. Castaneda, A. Silva, A. Gameiro, and M. Kountouris, "An Overview on Resource Allocation Techniques for Multi-User MIMO Systems", *IEEE Communications Surveys & Tutorials*, vol. 19, no. 1, pp. 239-284, 2017, doi: 10.1109/COMST.2016.2618870.

[8] K. -U. Storek and A. Knopp, "Fair User Grouping for Multibeam Satellites with MU-MIMO Precoding," *GLOBECOM 2017 - 2017 IEEE Global Communications Conference*, 2017, pp. 1-7, doi: 10.1109/GLOCOM.2017.8255098.

[9] D. G. Riviello, B. Ahmad, A. Guidotti and A. Vanelli-Coralli, "Joint Graph-based User Scheduling and Beamforming in LEO-MIMO Satellite Communication Systems," *2022 11th Advanced Satellite Multimedia Systems Conference and the 17th Signal Processing for Space Communications Workshop (ASMS/SPSC)*, 2022, pp. 1-8, doi: 10.1109/ASMS/SPSC55670.2022.9914723.

[10] Konc, Janez and Dušanka Janežič. "An improved branch and bound algorithm for the maximum clique problem", *MATCH - Communications in Mathematical and in Computer Chemistry*, vol. 58, no. 3, pp. 569-590, 2007.

[11] A. Guidotti and A. Vanelli-Coralli, "Design Trade-Off Analysis of Precoding Multi-Beam Satellite Communication Systems," *2021 IEEE Aerospace Conference (50100)*, 2021, pp. 1-12, doi: 10.1109/AERO50100.2021.9438169.

[12] 3GPP TR 38.821 V16.1.0, "Solutions for NR to support NON-terrestrial networks (NTN) (Release 16)", May 2021.

[13] 3GPP TR 38.811 V15.4.0, "Study on New Radio (NR) to support NON-terrestrial networks (Release 15)", Sep. 2020.

[14] Harry L. Van Trees, *Optimum Array Processing: Part IV of Detection, Estimation, and Modulation Theory*, John Wiley & Sons, 2004.

[15] G. Alfano, C.-F. Chiasserini, A. Nordio and D. G. Riviello, "A Random Matrix Model for mmWave MIMO Systems". *Acta Phys. Pol. B*, vol. 51, no. 7, pp. 1627-1640, 2020.

[16] J. E. Gentle, *Matrix algebra: theory, computations, and applications in statistics*, Springer Science & Business Media, 2007.

[17] P. Prosser, "Exact Algorithms for Maximum Clique: A Computational Study", *Algorithms* 2012, 5(4): 545-587, doi:10.3390/a5040545.

[18] A. Douik, H. Dahrouj, T. Y. Al-Naffouri and M. -S. Alouini, "A Tutorial on Clique Problems in Communications and Signal Processing", in *Proceedings of the IEEE*, vol. 108, no. 4, pp. 583-608, April 2020, doi: 10.1109/JPROC.2020.2977595.

[19] Z. O. Akbari, "A polynomial-time algorithm for the maximum clique problem", *2013 IEEE/ACIS 12th International Conference on Computer and Information Science (ICIS)*, 2013, pp. 503-507, doi: 10.1109/ICIS.2013.6607889.